Catalysis Today 141 (2009) 182–186

Contents lists available at ScienceDirect

Catalysis Today

journal homepage: www.elsevier.com/locate/cattod

Catalytic properties of nano-sized ZSM-5 aggregates

N. Viswanadham *, Raviraj Kamble, Madhulika Singh, Manoj Kumar, G. Murali Dhar

Catalysis and Conversion Process Division, Indian Institute of Petroleum, Dehradun 248005, India

ARTICLE INFO

Article history:
Available online 7 May 2008

Keywords:
ZSM-5
Mesoporosity
Micropore volume
t-Plot and adsorption isotherms

ABSTRACT

Nano-ZSM-5 (NZ) with well-defined porosity was synthesized by organic silica method. The material exhibited more than a twofold increase in pore volume when compared to the normal ZSM-5 (HZ). The increase in pore volume is observed in the entire range of the pores with diameter from 5 Å to 1500 Å. The order of increase in volume is macropores (>500 Å) > micropores (up to 20 Å) > mesopores (20–500 Å). Although macropore and mesopore formation is responsible for the major increase in the pore volume, significant increase in zeolitic pore volume was also observed in NZ. Both the ZSM-5 materials were tested for esterification of cyclohexanol with acetic acid under autogeneous pressure conditions where NZ showed better activity (69% conversion).

1. Introduction

Zeolites are finding more industrial applications by virtue of their properties such as thermal stability, shape selectivity, and the flexibility in tailor-making of catalyst for various reactions [1,2]. Presence of uniformly distributed micropores in the zeolites provides high surface area and excellent shape selectivity [3,4]. Y zeolite in fluid catalytic cracking (FCC), mordenite in *n*-paraffin isomerization and ZSM-5 in light alkane aromatizaton are some of the well-known industrial applications of zeolites [5–7]. However, the hydrothermally synthesized zeolites need to be modified to improve their properties especially for thermal stability, porosity, and acidity before their use for catalytic applications.

Steaming or acid treatment or combination of both treatments is generally used for the modification of zeolite properties [8–10]. The treatments facilitate removal of aluminum from the crystalline framework followed by its wash out by acid leaching to make more silicious zeolite. The type and severity of treatments needed for a zeolite depends on the zeolite types and the reaction to be catalyzed. In case of zeolite Y the steam dealumination is generally adopted for achieving the ultra stabilization [11]. In case of mordenite, the dealumination is used mainly for opening of the side pockets and for the creation of mesopores to improve the diffusion of bulky branched products [12,13]. For ZSM-5, the purpose is to improve its acidity as well as porosity [14]. Desilcation by post synthesis alkali treatment of silicious zeolites was also observed to create extra-porosity [15]. However, the materials obtained by such treatments may have limitations due to the presence of persistent extra-framework aluminum species in the narrow zeolite channels and structural damage of the framework at severe dealumination conditions [16,17]. The properties of the materials are also not reproducible at many times. Hence, it is recommended to tailor the zeolite properties during synthesis instead of its post synthesis modifications. Much work is done in the area of synthesizing large pore zeolites and high surface area mesoporous materials for obtaining the materials of improved porosity. But the industrial applications of these mesoporous materials are yet to be proven due to their lower thermal stability and weak acidity [18,19].

Creation of mesoporosity in zeolites such as ZSM-5 during hydrothermal synthesis is of much interest due to its wide applications in the petroleum, petrochemical, and fine chemical industries. More recently, a new carbon templating method has been introduced for creation of mesoporous voids in zeolites after the calcinations [20]. However, the method was reported to consume high amount of carbon material and limitations in incorporation of aluminum into the framework [21]. Grieken et al. reported the effect of synthesis parameters on the crystallinity and crystal size of the ZSM-5 [22]. Sorption isotherms, *t*-plots, cumulative pore volume curves, and pore size distribution data can provide useful information that can be used for tailor making of catalytic properties [23].

The present study is aimed to synthesize nanometer range ZSM-5 crystals with improved porosity, where detailed characterization studies such as surface area, external surface area, pore volume, micropore volume, mesoporosity, and the detailed pore size distributions were conducted to understand the properties of the new material. The material exhibited a twofold increase in pore volume due to the mesopores created at inter-crystalline voids and the increase in volume of zeolitic pores.

* Corresponding author.
E-mail addresses: nvish@iip.res.in, nviswanadham@india.com (N. Viswanadham).

0920-5861/$ – see front matter © 2008 Elsevier B.V. All rights reserved.
doi:10.1016/j.cattod.2008.03.026

2. Experimental

2.1. Zeolite synthesis

ZSM-5 zeolite of $SiO_2/Al_2O_3 = 60$ (HZ) was prepared by hydrothermal synthesis following inorganic silica source (sodium silicate) method [24]. Another method is used in the present study to obtain smaller ZSM-5 particles (nanometer range) using tetraethyl orthosilicate as silica source with controlled hydrolysis of silica, where the appropriate amount of aluminum nitrate (s.d. Fine Chemicals, India) was added to a 20 wt.% aqueous solution of tetrapropylammonium hydroxide (Merck), followed by stirring the mixture at 273 K to obtain clear solution. Appropriate amount of tetraethylortho-silicate was added to this solution and the mixture was stirred at room temperature for 40 h followed by heating at 353 K for obtaining super saturated solution. Zeolite crystallization was carried out in a teflon coated autoclave at 443 K for 48 h. The samples were dried at 383 K for 16 h followed by calcination at 773 K for 6 h.

2.2. Physico-chemical characterization

X-ray diffraction pattern of samples were recorded with a powder X-ray diffraction meter model Rigaku Dmax-III B. The measurements were conducted in a continuous $\theta/2\theta$ scan refraction mode using Cu Kα radiation. The anode was operated at 30 kV and 15 mA. The 2θ angles were measured from 5° to 60° at a rate of 2°/min.

Surface area and pore size distribution of samples were determined volumetrically by physisorption of nitrogen at liquid nitrogen temperature (77 K) in static mode using ASAP-2010 Micromeritics (USA) instrument. For all the samples, N_2 adsorption–desorption isotherms were obtained at 77 K and the temperature was maintained constant by using liquid nitrogen, whereas helium gas was used for measuring dead space. Surface area, pore volume and pore size distribution were obtained by measuring volume adsorbed at different P/P_0 values and by applying different methods. Total pore volume was estimated by measuring the volume of gas adsorbed at P/P_0 of 0.998, whereas, *t*-plot method was used to calculate the micropore surface area (<20 Å) using Harkins–Jura equation. The volume distribution in mesopores was obtained from the adsorption branch of the isotherm by applying BJH method. Total micropore volume (<20 Å) and, micropore size distribution were obtained using Horvath–Kawazoe method [20].

2.3. Catalytic activity

Esterification reaction was carried out in liquid phase batch reactor. The zeolite sample taken was 5 wt.% of cyclohexanol, and acetic acid and cyclohexanol were taken in 1:5 molar ratio. In a typical procedure, a 100-ml round bottom flask equipped with a water condenser and magnetic stirrer was kept in a constant temperature of oil bath. The reaction was carried out at atmospheric pressure at 100 °C. The reaction was conducted for about 10 h and samples were withdrawn from reaction mixture at regular intervals. The sample reaction mixture was chilled by ice to arrest the reaction. Further it was analyzed by HP Gas chromatograph. The conversion was calculated using the following formula:

$$\text{Conversion (wt.\%)} = 100 \times \frac{\text{initial wt.\% of cyclohexanol} - \text{final wt.\% of cyclohexanol}}{\text{initial wt.\% of cyclohexanol}}$$

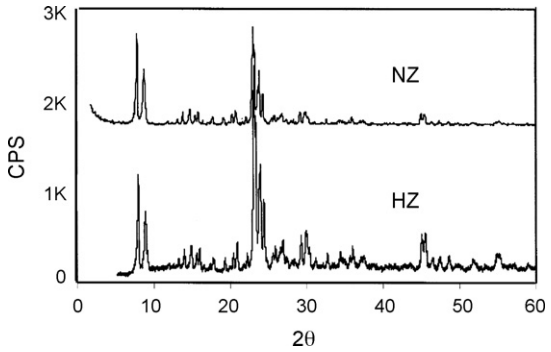

Fig. 1. X-ray diffraction patterns of ZSM-5 samples.

3. Results and discussion

The powder X-ray diffraction patterns of the samples are shown in Fig. 1. The samples exhibited the typical XRD patterns of ZSM-5 framework structure.

Table 1 also contains textural properties of zeolites. Significant difference in the properties of HZ and NZ samples was observed, where the sample NZ exhibited the higher surface area and pore volume. The BET surface area of HZ and NZ are 346 m^2/g and 461 m^2/g, respectively. The total pore volumes of the corresponding samples are 0.1763 cm^3/g and 0.3855 cm^3/g. The pore volume exhibited by HZ is in agreement with the literature findings [22,25]. The higher pore volume of NZ can be due to the increase in micropore, mesopore, and macropore volumes (Table 1). However, a careful analysis of the pore volume data indicated that the major increase in pore volume in NZ is due to the presence of pores with diameter > 500 Å, followed by the pores with diameter 20–500 Å.

Fig. 2 contains the adsorption–desorption isotherms of nitrogen at liquid nitrogen temperature. There is a significant difference in the shape of isotherms of both the samples. Sample HZ exhibited

Table 1
Surface area and pore volume properties of ZSM-5 samples

Sample	BET surface area (m^2/g)	Micropore area (m^2/g)	External surface area (m^2/g)	Total pore volume (cm^3/g)	Micropore volume (cm^3/g)
HZ	345.7	255.8	89.9	0.1763	0.1022
NZ	461.1	322.9	138.2	0.3855	0.1321

Pore size distribution						
Volume in pores of diameter (Å)						
	Up to 10	10–20	20–100	100–200	200–500	>500
HZ	0.1262	0.0134	0.0143	0.0039	0.0079	0.0105
NZ	0.1637	0.0261	0.0176	0.0097	0.0220	0.1464
Increase in pore volume (NZ–HZ)	0.0375	0.0127	0.0033	0.0058	0.0141	0.1359
% Increase in pore volume of NZ	18.0	6.0	1.5	2.7	6.6	65.2
% Increase in types of pores (volume)	Micropore 24.0		Mesopore (10–500 Å) 10.8			Macropore 65.2

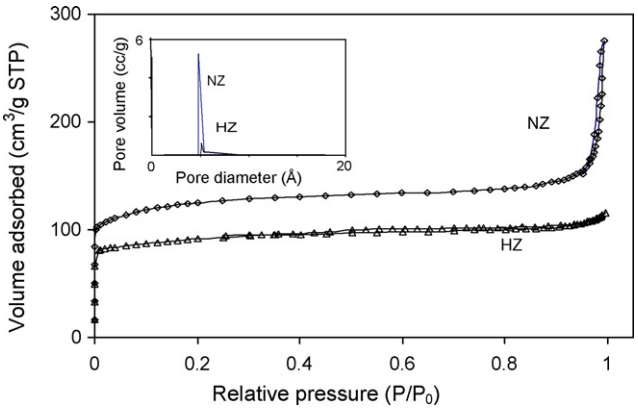

Fig. 2. Adsorption desorption isotherms of ZSM-5 samples. Inset: Horvath–Kawazoe differential pore volume plots.

type I isotherm according to IUPAC classification which is characteristic of microporous material [26]. However, presence of a very small hysteresis loop which closes at P/P_0 of ~0.4 indicates the presence of slit-shaped inter-crystalline void in HZ. For the sample NZ, the hysteresis loop of nitrogen appears at very high relative pressure (P/P_0 = 0.9–1.0) related to the capillary condensation in inter-crystalline macropores created by agglomeration of small particles [27]. It can be seen that this sample possess both micro-and mesoporous features. The rise of sorption at $P/P_0 < 0.05$ is corresponds to the micropore filling of the zeolite.

Detailed analysis of micropore size distribution can be done from Horvath–Kawazoe diffusion pore volume plot in Fig. 2 inset. The pore diameter of ~5.5 Å indicated the zeolitic pores of ZSM-5. Both the samples exhibited a sharp peak around 5.5 Å correspond to ZSM-5. However, distinct increase in peak area of the micropore volume of NZ is noticed, i.e., 0.8 cm^3/g Å of HZ to 5.5 cm^3/g Å of NZ. That means there is an improvement in the zeolitic pores of ZSM-5 synthesized by the new method (NZ).

The *t*-plot method is used for the determination of external surface area, micropore surface area, and micropore volume [28]. Fig. 3 contains the *t*-plot of the samples, where NZ indicated higher micropore volume compared to that of HZ. The surface area was also increased in the samples NZ (Table 1).

BJH pore size distribution curves of the samples given in Fig. 4 also indicate the presence of higher mesopore volume in sample NZ. A careful analysis of the curve indicates that the sample NZ has significant number of mesopores as well as macropores when compared to HZ. The creation of these meso and macropores can be ascribed to the presence of inter-crystalline voids in the sample NZ.

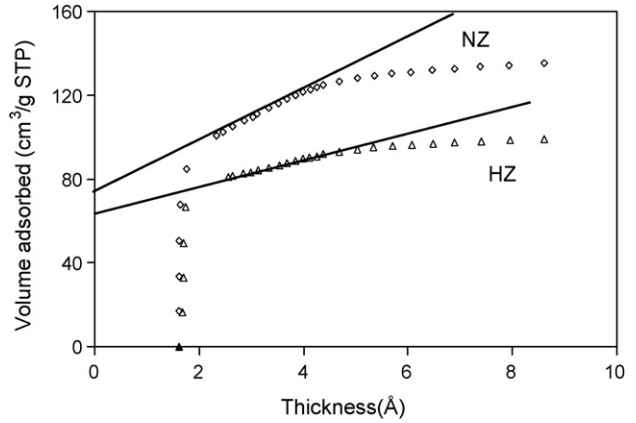

Fig. 3. *t*-Plots of the ZSM-5 samples.

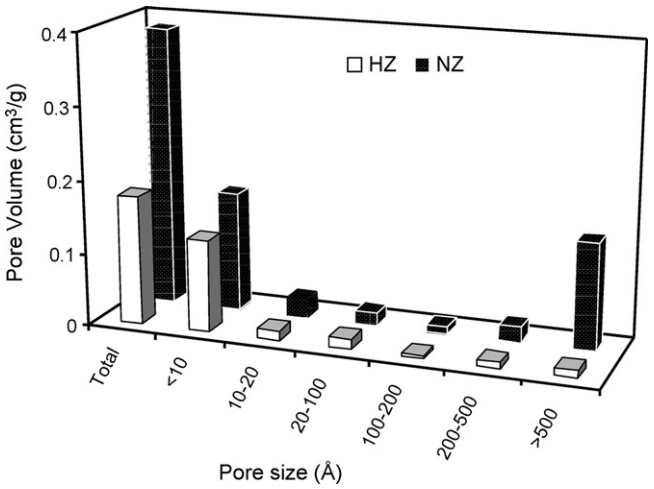

Fig. 4. BJH pore size distribution curves.

The range of pore diameters obtained in meso and macropore region of the NZ indicates the presence of nano-particles of varying size. The pore volume of NZ was also more in the micropore region (detailed range of micropore volume is not covered in this graph). The results obtained from Hovath–Kowazoe and BJH method have been used for the calculation of the entire range of pore size distribution covering the micropores as well as mesopores of the samples HZ and NZ. Based on these values a pore size distribution histogram is made in Fig. 5. The histogram provides a quantitative measure to understand the contribution of pores of various diameters to the pore volume of the samples. The total pore volume of NZ and HZ are 0.3855 cm^3/g and 0.1763 cm^3/g, respectively (Table 1). The difference in pore volume indicates significant increase (0.2092 cm^3/g) in pore volume of NZ (almost double to that of HZ). Among the pores of various diameters, the macropore of >500 Å contributed to the major increase in the pore volume of NZ, followed by micropores (up to 20 Å). There is also a marginal increase in volume of mesopores of 20–500 Å diameter range. The volume increase in pores of various diameter in the NZ sample are 0.0375, 0.0127, 0.0033, 0.0058, 0.0141, and 0.1359 for the pores of diameter up to 10 Å, 10–20 Å, 20–100 Å, 100–200 Å, 200–500 Å, and above 500 Å, respectively. The percentage increase in the pore volume of the corresponding pores is 18.0%, 6.0%, 1.5%, 2.7%, 6.6%, and 65.2%, respectively (Table 1). Thus the order of pore volume increase can be represented as "above 500 Å > up to

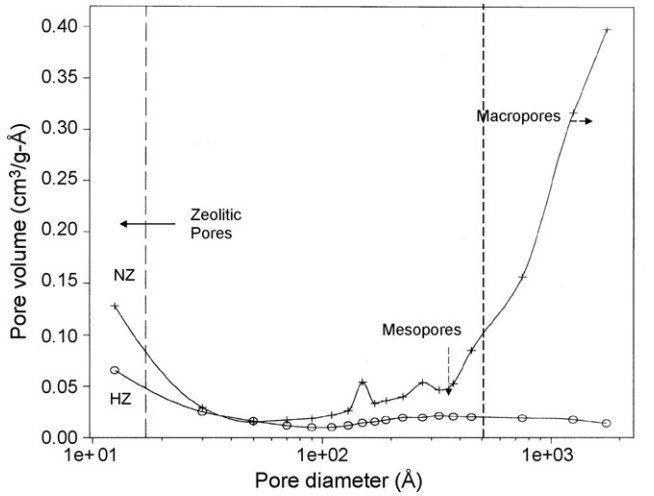

Fig. 5. Pore volume and pore size distribution in ZSM-5 samples.

10 Å > 200–500 Å > 10–20 Å > 100–200 Å > 20–100 Å". It is important to note that the increase in macropore volume in pores of diameter > 500 Å is as high as 64.0% of the total increase in pore volume. In order to see the contribution of individual pores to the total pore volume, the entire range of pores can be classified as (a) micropores (up to 20 Å), (b) mesopores (20–500 Å), and macropores (>500 Å). The increase in volume in pores of each type has been calculated by subtracting the pore volumes of HZ from those of NZ. The data obtained indicated that the increase in the micro, meso, and macropore volume of NZ is 24%, 11%, and 65%, respectively. The order of increase in pore volume can be given as macro > micro > meso. The NZ sample with increased porosity is expected to exhibit improved diffusion of the molecules in hydrocarbon conversion reactions.

The presence of mesopore and macropores in the NZ may be due to the inter-particle voids of the zeolite nano-particles. Camblor et al. reported that in case of nano-Beta zeolite, increased external surface area was observed with the decrease of particle size. It has been demonstrated that with decrease of the crystal sizes from 200 nm to 10 nm the micropore volume systematically decreases as well [29]. This observed tendency is apparent below 100 nm crystal size, and becomes striking for crystal having sizes smaller than 50 nm. The increase in external surface area of nano-size Beta crystals is understood by the increased surface of the crystallites with decreasing particle size. But, the decrease in micropore volume cannot be explained by the same reason. However, the decrease in the micropore volume in case of Beta zeolite was attributed to the occupation of nano-crystalline domains in Beta zeolite particles. The studies of Fojtikova et al. on micro/meso composite material also indicated the phenomenon of increase in external surface area with the decreasing crystal size of nano-ZSM-5 [27]. The higher external surface area was also reported in case of nano-silicalite particles [30]. Song et al. have established the relation between crystal size of ZSM-5 and external surface area, where a sharp increase in external surface area occurs at crystal size going below 100 nm [30].

A commonality observed in all the above mentioned studies is the increase in external surface area of the zeolite samples with the decrease in the crystal size. Based on this theory, the higher external surface area values of NZ (138.2 m^2/g) when compared to HZ (89.9 m^2/g) observed in the present study can be explained by the possible formation of nano-ZSM-5 particles in the NZ sample. Based on the standard curve of external surface area and particle size proposed by Song et al., the external surface area value of ~138 m^2/g observed in NZ sample of the present study represents the crystal size of about 1150 nm. SEM image of sample also indicated the formation of small crystals in sample NZ (Fig. 6). Camblor's study indicated the decrease in micropore volume of nano-sized Beta zeolite. However, no decrease in micropore volume of the NZ when compared to the HZ was observed in the present study. Song et al. also did not report the decrease in micropore volume of the nano-silicalite. The ZSM-5 reported in present study and the silicalite reported by Song et al. differs from the decrease in micropore volume of Beta proposed by Camblor et al. [29]. On the other hand, the sample NZ of the present study exhibited much higher micropore volume (0.1321 cm^3/g) than HZ (0.1022 cm^3/g). The differences in micropore volume of NZ of the present study with that of the Beta zeolite may be due to the difference in the pore system and particle size of the two zeolites. In case of Beta zeolite, the nano-crystalline domains occupied the micropores of Beta zeolite particles to decrease the micropore volume. The NZ particles of the present study seem to be bigger than the diameter of the zeolite micropores, and hence, no loss in micropore volume is observed. Rather, a twofold increase in micropore volume (up to 20 Å) of NZ was observed. Moreover, the mesopore and macropore volume also increased in NZ. This can be possible by the formation of the inter-crystlline voids of different size probably facilitated by the aggregation of the nano-particles of different sizes. Absence of any non-crystalline/amorphous material in zeolitic pores of NZ may also be responsible for the increase in micropore volume in the present study. Studies of Song et al. revealed the lower intensities and higher line width of the XRD patterns of the silicalite with decreasing crystallite size [30]. Based on this, the lower intensity of XRD patterns of the NZ (at $2\theta = 22^\circ$–26°) observed in the present study (Fig. 1) can be ascribed to the formation of smaller zeolite crystals in NZ.

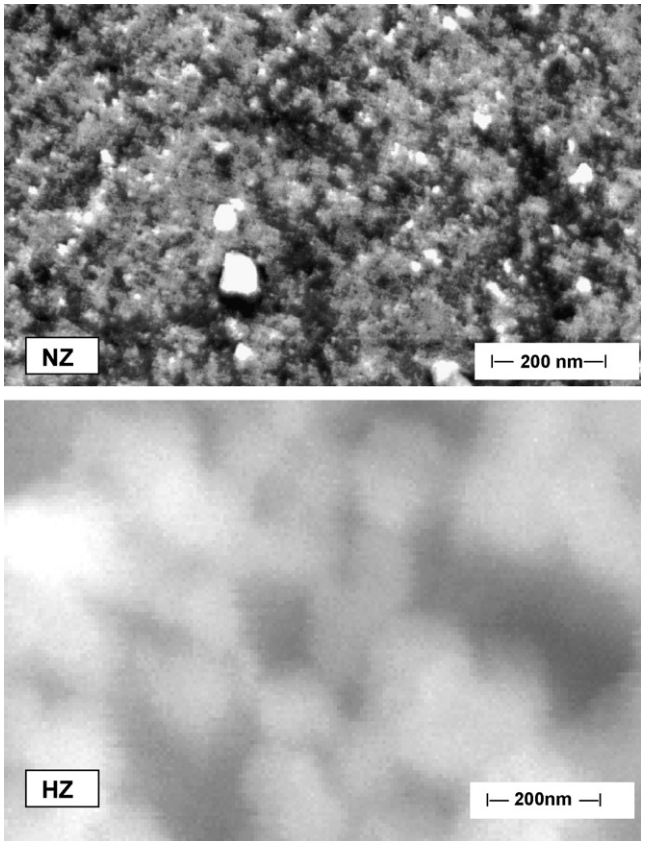

Fig. 6. Scanning electron micrographs (SEM) of ZSM-5 samples.

The esterification reaction of cyclcohexanol and acetic acid was carried out as model reaction to test the activity of zeolite samples. The product obtained is cyclohexyl acetate which is one of the industrially important flavour. The reaction is very slow without catalyst and the rate can be accelerated by acid catalyst. The

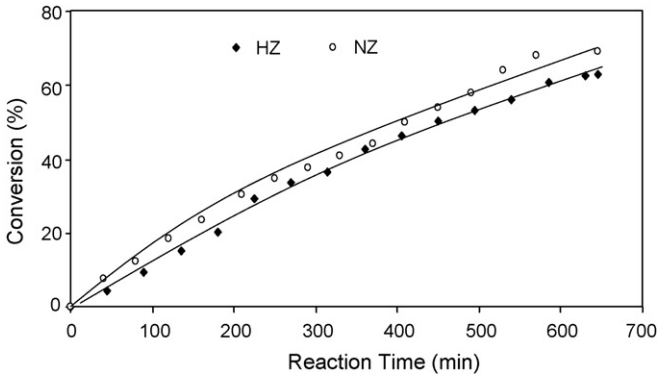

Fig. 7. Catalyst performance of ZSM-5 zeolites in esterification.

reaction conditions maintained were same for each catalyst which would help to understand the performance of catalyst. The performance of catalyst can be understood from Fig. 7.

The activity of NZ and HZ can be compared as both have nearly same Si/Al ratios. From Fig. 7, it becomes clear that the NZ showed much higher activity than HZ. The maximum conversion found in case of NZ is 69% whereas it is 63% for HZ. This activity difference indeed can be attributed to the large surface area and high pore volume present in nano-sized ZSM-5 catalyst.

Overall, the present study indicated the improvement in micropore, mesopore, and macropore volumes of the ZSM-5 with decrease in crystal size. Increase in mesoporosity is in agreement with the earlier literature findings [27–31]. But, increase in micropore volume was not reported so far for the mesoporous zeolites such as Beta, silicalite, mordenite, and ZSM-5. Rather, decrease in micropore volume of the Beta zeolite was reported. This difference may be due the difference in pore type of the zeolites and the difference in the synthesis procedure. Differences in the synthesis procedures were also observed to affect the properties of zeolites. Effect of synthesis method and the crystallization time on the crystal size of ZSM-5 was well studied. A detailed mechanism for the transformation of precursors into nano-slabs from the TPAOH-TEOS-H_2O system was indeed reported by Kirschhock et al. [32,33]. Their studies indicated the increase in crystallinity of ZSM-5 with crystallization time up to 48 h. Further increase in synthesis time above 48 h was reported to cause the formation of bigger ZSM-5 crystals. The studies indicated the importance of the control on crystallization time to obtain the desired particle size of the ZSM-5. We believe that the reaction conditions adopted for the synthesis of NZ in the present study are suitable for the creation of pores in the entire range of micro, meso and macropore region. The ZSM-5 (NZ) with higher surface area and pore volume obtained in the present study is expected to exhibit improved catalytic activity and slow deactivation rates in the esterification and other hydrocarbon conversion reactions [31].

4. Conclusions

TEOS method can be used for obtaining the ZSM-5 of improved porosity with increase in zeolitic pores as well as the creation of mesopores. The external surface area values and SEM results support the formation of much smaller ZSM-5 crystals in NZ sample than in the HZ, a possible source for the formation of intercrystalline voids in the range of mesopores. The NZ exhibits improved catalytic activity in esterification reaction due to the improved porosity and more strong acid sites.

Acknowledgements

Our sincere thanks to SEM analysis group at Wadia Institute of Himalayan Geology and the Director, IIP, for his encouragement to carryout fundamental research. One of us (RK) acknowledges CSIR for awarding JRF fellowship.

References

[1] H.L. Hoffman, Hydrocarb. Process 67 (2) (1987) 41.
[2] W. HÖlderich, M. Hesse, F. Naumann, Angew. Chem. Int. Edit. Engl. 27 (1988) 226.
[3] A. Hollo, Appl. Catal. 229 (2000) 93.
[4] N.Y. Chen., W.E. Garwood, Catal. Rev. Sci. Eng. 28 (2&3) (1986) 198.
[5] M.A. Camblor, A. Corma, A. Martinez, F.A. Mocholi, J.P. Pariente, Appl. Catal. 35 (1987) 299.
[6] N. Viswanadham, J.K. Gupta, L Dixit, M.O. Dixit Garg, J. Mol. Catal. 258 (2006) 15.
[7] N. Viswanadham, G. Muralidhar, T.S.R. Prasada Rao, J. Mol. Catal. 223 (2004) 269.
[8] J. Scherzer, ACS Sym. Ser. 248 (1984) 157.
[9] Y.H. Shou, C.S. Cundy, A.A. Garforth, V.L. Zholobenko, Microporous Mesoporous. Mater. 89 (2006) 78.
[10] S. van Donk, A.H. Janssen, J.H. Bitter, K.P. de Jong, Catal. Rev. 45 (2003) 297.
[11] A.H. Janssen, A.J. Koster, K.P. de Jong, Angew. Chem. Int. Edit. 40 (2001) 1102.
[12] N. Viswanadham, M. Kumar, Microporous. Mesoporous. Mater. 92 (2006) 31.
[13] M.J.A. van Tromp, M.T. Garriga Oostenbrink, J.H. Bitter, K.P. de Jong, D.C. Koningsberger, J. Catal. 190 (2000) 209.
[14] J.L. Molz, H. Heinichen, W.F. HÖlderich, J. Mol. Catal. A: Chem. 136 (1998) 175.
[15] J.C. Groen, J.C. Jansen, J.A. Moulijn, J. Pe'rez-Ramirez, J. Phys. Chem. B 108 (2004) 13062.
[16] N. Viswanadham, N. Ray, T.S.R. Prasada Rao, Stud. Surf. Sci. Catal. 113 (1998) 433.
[17] (a) N. Viswanadham, T. Uday, L. Dixit, Am. Chem. Soc. Div. Fuel. Chem. Prepr. 48 (2) (2003) 868;
(b) T.S.R. Prasada Rao, N. Viswanadham, G. Murali Dhar, N. Ray, Shapelective catalysis in hydrocarbon processing and Chemicals synthesis, in: C. Song, J. Graces, Y. Sugi (Eds.), 1999.
[18] Z.H. Luan, C.F. Cheng, H.Y. He, J. Klinowsky, J. Phys. Chem. 99 (1995) 10590.
[19] A. Corma, M.S. Grande, V. Gonzalez Alfaro, A.V. Orchilles, J. Catal. 159 (1996) 375.
[20] J. Schmidt, A. Boisen, E. Gustavssion, K. Stahl, S. Pehrson, S. Dahl, A. Carlsson, C.J.H. Jacobsen, Chem. Mater. 13 (2001) 4416.
[21] F.A. Topsoe, C.J.H. Jacobson, M. Brorson, C. Madsen, F. Schmidt, US Patent 6,241,960, (1999).
[22] R. Van Grieken, J.L. Sotelo, J.M. Menéndez, J.A. Melero, Micropor. Mesopor. Mater. 39 (2000) 135.
[23] M. Jaroniec, K. Kaneko, Langmuir 15 (1997) 6589.
[24] R.J. Argauer, G.R. Landolt, US Patent 3,702,886, (1972).
[25] N. Viswanadham, G. Murali Dhar, T.S.R. Prasada Rao, J. Mol. Catal. A 125 (1997) L87.
[26] A.E. Persson, B.J. Schoeman, J. Sterte, J.E. Otterstedt, Zeolites 14 (1994) 314.
[27] P.P. Fojtíková, S. Mintova, J. Čejka, N. Žilková, A. Zukal, Micropor. Mesopor. Mater. 92 (2006) 154.
[28] B.C. Lippes, J.H. de Boer, J. Catal. 4 (1965) 319.
[29] M.A. Camblor, A. Corma, S. Valencia, Micropor. Mesopor. Mater. 29 (1998) 59.
[30] W. Song, R.E. Justice, C.A. Jones, V.H. Grassian, S.C. Larsen, Langmuir 20 (2004) 4696.
[31] R. Srivastava, M. Choi, R. Rayoo, Chem. Commun. (2006) 4489.
[32] C.E.A. Kirschhock, R. Ravishankar, L. Van Looveren, P.A. Jacobs, J.A. Martens, J. Phys. Chem. B 103 (1999) 4972.
[33] C.E.A. Kirschhock, R. Ravishankar, P.A. Jacobs, J.A. Martens, J. Phys. Chem. B 103 (1999) 11021.